J. Fluid Mech. (1973), *vol.* 58, *part* 2, *pp.* 263–273
Printed in Great Britain

Effects of finite conductivity in linearized magnetogasdynamic flows

By SHIGEKI MORIOKA AND TOSHISADA MIKI
Faculty of Engineering Science, Osaka University, Japan

(Received 12 December 1972)

The steady flow of an ideal gas with finite conductivity past a thin wedge section in an aligned magnetic field is considered within the linearized theory. The wedge is assumed to be an insulator or a perfect conductor. The flow field around the obstacle is found by numerical integration of the Fourier transform for various values of the Mach number, the Alfvén Mach number and the magnetic Reynolds number in the main stream. The outer flow is estimated by the method of asymptotic expansions. These results disclose how the inner flow including gasdynamic features changes to the magnetohydrodynamic outer flow.

1. Introduction

This paper is concerned with the linearized theory of steady flow of a compressible fluid with finite conductivity past a thin cylindrical obstacle in the presence of an aligned magnetic field. The similar problems for an incompressible fluid have been investigated extensively (e.g. Sears & Resler 1959), while those for a compressible fluid are restricted to the cases of extremely high or low magnetic Reynolds number (McCune & Resler 1960; Imai 1960; Sakurai 1960; Tamada 1962) or a special configuration such as the flow past a sinusoidal wall (Resler & McCune 1960).

The flow field of a compressible fluid with finite conductivity can be characterized by the Mach number M, the Alfvén Mach number A and the magnetic Reynolds number R_m in the main stream. Then, in the limit of ordinary gasdynamics $R_m \to 0$, the flow is of the hyperbolic type only for $M > 1$ and has a shock wave. But, in the opposite limit $R_m \to \infty$, the flow becomes elliptic in type for $A < 1$ even if $M > 1$, and a weak shock is impossible, while it becomes hyperbolic in type for $A < 1$ and $M^2 + A^2 > 1$ even if $M < 1$, and an upstream shock is possible. For $M > 1$ and $A > 1$, the flow field is of the hyperbolic type in both limits, but their characteristic curves have different directions. Thus it is very interesting to see how different types of flow are connected for different limiting values of R_m.

For this purpose, we consider a steady two-dimensional flow of an ideal gas with finite conductivity past a simple wedge with a small angle and a finite length followed by a straight section. The magnetic field is assumed to be aligned. Such a special type of obstacle is chosen because it gives the simplest physically meaningful flow and does not cause a restriction on the analysis.

Such a magnetohydrodynamic problem can be dealt with conveniently by the Fourier transform technique, and the solutions can be obtained in Fourier integral form in general. It is difficult, however, to deduce the flow properties from them directly, because of the complicated integrand including the roots of a characteristic equation with complex coefficients. At the present time, however, it is comparatively easy to evaluate such an integral by making use of a computer. These numerical results, as well as the knowledge of the outer flow estimated by the method of asymptotic expansions, serve to find the effects of finite conductivity on the compressible flow mentioned above.

2. Basic equations

The basic equations describing a linearized two-dimensional compressible flow with an aligned magnetic field have been provided by many authors (e.g. McCune & Resler 1960). We choose the origin of the co-ordinate system at the nose and the x axis along the main stream and hence the centre-line of the wedge section, and the y axis perpendicular to it. The distance between the nose and the shoulder is taken as the scale length. The x and y components of the perturbation velocity and magnetic field are denoted by u, v, B_x and B_y, respectively. They are normalized by their values in the main stream. Then, these quantities are related by the following equations:

$$(1-M^2)\frac{\partial u}{\partial x}+\frac{\partial v}{\partial y}=0, \tag{1}$$

$$\frac{\partial v}{\partial x}-\frac{\partial u}{\partial y}=N(B_y-v), \tag{2}$$

$$\frac{\partial B_x}{\partial x}+\frac{\partial B_y}{\partial y}=0, \tag{3}$$

$$\frac{\partial B_y}{\partial x}-\frac{\partial B_x}{\partial y}=R_m(B_y-v), \tag{4}$$

where $N = R_m/A^2$ denotes the interaction parameter. The dimensionless perturbation pressure and density then can be expressed in terms of u:

$$p=-\gamma M^2 u, \quad \rho=-M^2 u, \tag{5}$$

where γ is the ratio of the specific heats.

Since the flow is symmetric about the x axis, only the flow in the upper half-plane will be considered in the following description. A part of the boundary conditions is given by the requirement that all the perturbation quantities vanish at infinity and that the fluid flows along the surface of the obstacle:

$$u=v=B_x=B_y=0 \quad \text{as} \quad y\to\infty, \tag{6}$$

$$v=\tfrac{1}{2}[\operatorname{sgn}(x)-\operatorname{sgn}(x-1)] \quad \text{as} \quad y=0. \tag{7}$$

The remaining condition depends on the behaviour of the magnetic field at the surface and it differs according to whether the obstacle is an insulator or a conductor. For a symmetric insulator, we have

$$B_y=0 \quad \text{at} \quad y=0. \tag{8a}$$

At this point, we can show that the y component of the magnetic field is of second order throughout the obstacle, by solving for the magnetic field inside the insulator as a perturbation of the main field and by taking account of its symmetry about the x axis. Also we can show that the x component retains its surface value throughout the obstacle, by matching continuously to the outer field. On the other hand, for the ideal obstacle consisting of a perfect conductor, we have

$$B_y = v \quad \text{at} \quad y = 0. \tag{8b}$$

This means that the line of force cannot penetrate into the perfect conductor and runs along its surface. A sheet current of zeroth order proportional to the surface field then flows along the surface.

3. Solution in Fourier integral form

We use Fourier transforms with respect to x to solve (1)–(8). Transformed quantities are distinguished from the original physical quantities by adding an overbar, e.g.

$$\bar{v}(\xi, y) = \frac{1}{(2\pi)^{\frac{1}{2}}} \int_{-\infty}^{\infty} v(x, y)\, e^{-i\xi x}\, dx. \tag{9}$$

By eliminating all the quantities except $\bar{v}$ among the transformed equations, the following equations are obtained:

$$\frac{d^4\bar{v}}{dy^4} - i\xi[(m-1)\, i\xi + \beta]\frac{d^2\bar{v}}{dy^2} + i\xi^3(mi\xi - \alpha)\,\bar{v} = 0, \tag{10}$$

$$\bar{v} = 0 \quad \text{as} \quad y \to \infty, \tag{11}$$

$$\bar{v} = \frac{1}{(2\pi)^{\frac{1}{2}} i\xi}(1 - e^{-i\xi}) \quad \text{as} \quad y = 0, \tag{12}$$

$$\frac{1}{mi\xi}\frac{d^2\bar{v}}{dy^2} - (\sigma N + i\xi)\,\bar{v} = 0 \quad \text{as} \quad y = 0, \tag{13}$$

where $m = M^2 - 1$, $\alpha = N(M^2-1)(A^2-1)$ and $\beta = N(M^2 + A^2 - 1)$. The index σ takes the value 1 or 0 according as the obstacle is an insulator or perfect conductor. The transforms of the other quantities can be expressed in terms of $\bar{v}$:

$$\bar{u} = (mi\xi)^{-1}\, d\bar{v}/dy, \tag{14}$$

$$N\bar{B}_x = -\frac{1}{m\xi^2}\frac{d^3\bar{v}}{dy^3} - \frac{N + i\xi}{i\xi}\frac{d\bar{v}}{dy}, \tag{15}$$

$$N\bar{B}_y = -\frac{1}{mi\xi}\frac{d^2\bar{v}}{dy^2} + (N + i\xi)\,\bar{v}. \tag{16}$$

The solution satisfying (10)–(13) can be expressed as follows:

$$\bar{v} = [V_1 \exp(y\lambda_1) + V_2 \exp(y\lambda_2)](1 - e^{-i\xi}), \tag{17}$$

$$V_1 = \frac{\lambda_2^2 + m\xi^2 - \sigma ni\xi}{(2\pi)^{\frac{1}{2}} i\xi(\lambda_2^2 - \lambda_1^2)}, \quad V_2 = -\frac{\lambda_1^2 + m\xi^2 - \sigma ni\xi}{(2\pi)^{\frac{1}{2}} i\xi(\lambda_2^2 - \lambda_1^2)}, \tag{18}$$

$$\left.\begin{aligned}\lambda_1 &= \pm\xi\left[-\left(\frac{m-1}{2}+\frac{\beta}{2i\xi}\right)+\left\{\left(\frac{m-1}{2}+\frac{\beta}{2i\xi}\right)^2+\left(m-\frac{\alpha}{i\xi}\right)\right\}^{\frac{1}{2}}\right]^{\frac{1}{2}},\\ \lambda_2 &= \pm\xi\left[-\left(\frac{m-1}{2}+\frac{\beta}{2i\xi}\right)-\left\{\left(\frac{m-1}{2}+\frac{\beta}{2i\xi}\right)^2+\left(m-\frac{\alpha}{i\xi}\right)\right\}^{\frac{1}{2}}\right]^{\frac{1}{2}},\end{aligned}\right\} \tag{19}$$

where $n = Nm$, and the $\pm$ signs in (19) must be chosen such that the real parts of λ_1 and λ_2 are negative.

The corresponding physical quantities can be found by taking the inverse transforms of (17) and (14)–(16). For instance,

$$\begin{aligned} v &= \frac{1}{(2\pi)^{\frac{1}{2}}}\int_{-\infty}^{\infty}\bar{v}\,e^{ix\xi}\,d\xi \\ &= \sum_{s=1,2}\left[\frac{1}{\pi}\int_0^{\infty}\exp(y\lambda_{sr})\{V_{sr}\cos(x\xi+y\lambda_{si})-V_{si}\sin(x\xi+y\lambda_{si})\}\,d\xi\right. \\ &\quad \left.-\frac{1}{\pi}\int_0^{\infty}\exp(y\lambda_{sr})\{V_{sr}\cos(x\xi-\xi+y\lambda_{si})-V_{si}\sin(x\xi-\xi+y\lambda_{si})\}\,d\xi\right], \end{aligned} \tag{20}$$

where λ_{sr} and λ_{si} $(s = 1, 2)$ denote the real and the imaginary parts of λ_s, and V_{sr} and V_{si} the real and the imaginary parts of $(2\pi)^{\frac{1}{2}}V_s$. The first integral in the right-hand side of (20) expresses the compression effect due to the nose and the second the expansion effect due to the shoulder. Similar expressions can be obtained for the other quantities.

4. Asymptotic expression of the solution

Since λ_{sr} in (20) does not vanish in general, the asymptotic expression of the integral can be found for large values of y according to the Laplace's method (Erdélyi 1956, p. 36). The major contribution to the value of the integral arises from the immediate vicinity of those points of the interval $0 \leqslant \xi < \infty$ at which $\lambda_{sr}(\xi)$ assumes its largest value. Now the largest value of $\lambda_{sr}(\xi)$ arises at $\xi = 0$, as may be seen from (19), and the asymptotic expression can be provided by expanding λ_{sr}, λ_{si}, V_{sr} and V_{si} in the neighbourhood of $\xi = 0$.

First we consider the case of $\alpha/\beta > 0$. This case yields a hyperbolic type of flow in the limit $R_m \to \infty$. Then in the neighbourhood of $\xi = 0$, λ_{sr}, λ_{si}, V_{sr} and V_{si} are expanded as follows:

$$\left.\begin{aligned}\lambda_{1r} &= -(\tfrac{1}{2}|\beta|)^{\frac{1}{2}}\xi^{\frac{1}{2}}+O(\xi^{\frac{3}{2}}),\\ \lambda_{1i} &= -\operatorname{sgn}(\beta)(\tfrac{1}{2}|\beta|)^{\frac{1}{2}}\xi^{\frac{1}{2}}+O(\xi^{\frac{3}{2}}),\end{aligned}\right\} \tag{21}$$

$$\left.\begin{aligned}\lambda_{2r} &= -\left|\left(\frac{\alpha}{\beta}\right)^{\frac{1}{2}}\frac{1}{2\alpha}\left(m-\frac{\alpha}{\beta}\right)\left(1+\frac{\alpha}{\beta}\right)\right|\xi^2+O(\xi^4),\\ \lambda_{2i} &= -\operatorname{sgn}(m)(\alpha/\beta)^{\frac{1}{2}}\xi+O(\xi^3),\end{aligned}\right\} \tag{22}$$

$$\left.\begin{aligned}V_{1r} &= O(1), \quad V_{1i} = -\sigma n/\beta\xi+O(\xi),\\ V_{2r} &= O(1), \quad V_{2i} = -(1-\sigma n/\beta)/\xi+O(\xi).\end{aligned}\right\} \tag{23}$$

The major contribution to the integral of (20) comes from the terms involving V_{2i}. On taking into account only the first terms in (22) and (23), we obtain the following asymptotic expression:

$$v = \frac{1}{2}\left(1-\sigma\frac{n}{\beta}\right)\left[\operatorname{erf}\left\{\frac{x-\operatorname{sgn}(m)\,(\alpha/\beta)^{\frac{1}{2}}y}{2\Gamma y^{\frac{1}{2}}}\right\}-\operatorname{erf}\left\{\frac{x-1-\operatorname{sgn}(m)\,(\alpha/\beta)^{\frac{1}{2}}y}{2\Gamma y^{\frac{1}{2}}}\right\}\right], \tag{24}$$

where

$$\Gamma = \left|\left(\frac{\alpha}{\beta}\right)^{\frac{1}{2}}\frac{1}{2\alpha}\left(m-\frac{\alpha}{\beta}\right)\left(1+\frac{\alpha}{\beta}\right)\right|^{\frac{1}{2}} = \frac{2^{\frac{1}{2}}M^2A^2|M^2-1|^{\frac{1}{4}}}{R_m^{\frac{1}{2}}(M^2+A^2-1)^{\frac{5}{4}}|A^2-1|^{\frac{1}{4}}}. \tag{25}$$

The factor Γ is useful to estimate the possibility of an observation of magnetohydrodynamic shock. If this factor is sufficiently small compared with unity, then the observation of a magnetohydrodynamic shock wave will be possible. Equation (24), however, does not provide the correct value in the limit $R_m \to \infty$ for the insulator ($\sigma = 1$). It may be small if n/β is positive or large if n/β is negative. In this limit, however, the flow near the obstacle is considerably decelerated owing to the strong Lorentz force, if the condition (8*a*) is accepted, and the linearized theory is no longer applicable. In fact, from the Fourier integral of u, we can deduce that the perturbation velocity diverges and is proportional to $N^{\frac{1}{2}}$ in the neighbourhood of the obstacle. For the perfect conductor ($\sigma = 0$), on the other hand, the linearized theory is valid for all values of R_m, and the asymptotic expression (24) also provides the correct value at the limit of $R_m \to \infty$.

In the gasdynamic limit $R_m \to 0$, the appropriate expansion of the Fourier integral (20) may be obtained from the expansion with respect to small N, rather than small ξ. Thus we can show that (20) reduces to the solution of the ordinary gasdynamic flow at this limit, for both the insulator and the perfect conductor.

For the case of $\alpha/\beta < 0$, which yields an elliptic type of flow in the limit $R_m \to \infty$, only equation (22) must be changed, to

$$\left.\begin{aligned}\lambda_{2r} &= -|\alpha/\beta|^{\frac{1}{2}}\xi + O(\xi^3),\\ \lambda_{2i} &= \left|\frac{\alpha}{\beta}\right|^{\frac{1}{2}}\frac{1}{2\alpha}\left(m-\frac{\alpha}{\beta}\right)\left(1+\frac{\alpha}{\beta}\right)\xi^2 + O(\xi^4).\end{aligned}\right\} \tag{26}$$

The major contribution to the integral arises from the terms involving V_{2i} again, and we have the following asymptotic expression:

$$v = \left(1-\sigma\frac{n}{\beta}\right)\frac{1}{\pi}\left\{\tan^{-1}\frac{x}{|\alpha/\beta|^{\frac{1}{2}}y} - \tan^{-1}\frac{x-1}{|\alpha/\beta|^{\frac{1}{2}}y}\right\}. \tag{27}$$

Equation (27) does not provide the correct asymptotic value in the limit $R_m \to \infty$ for the insulator, for the same reason as that mentioned previously.

5. Numerical results and discussion

The flow field comparatively near the obstacle can be found by numerical calculation of the Fourier integrals. Using a computer, we can find the roots of the characteristic equation with complex coefficients and evaluate the integrals including their roots.

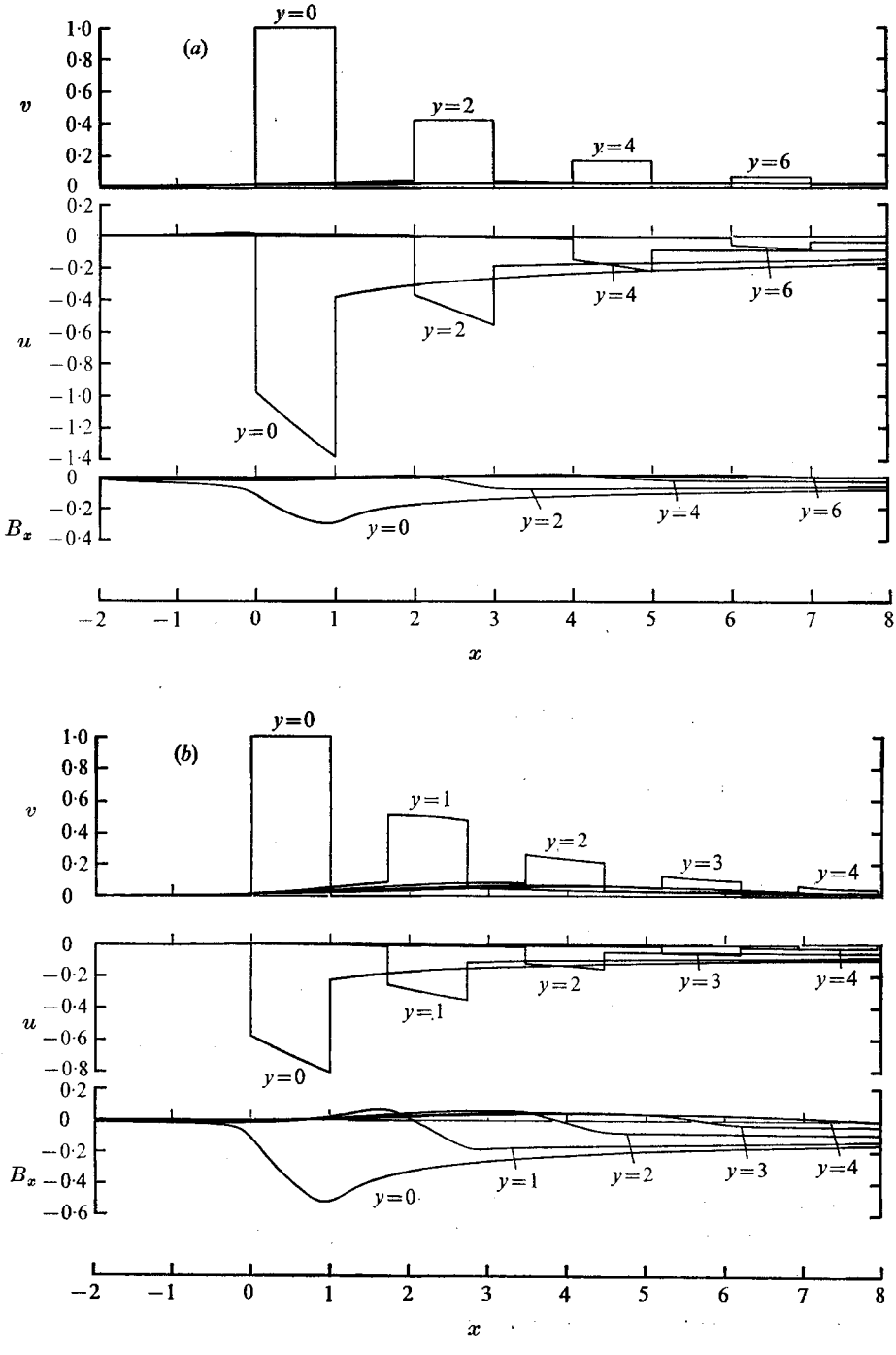

FIGURES 1 (*a*, *b*). For legend see facing page.

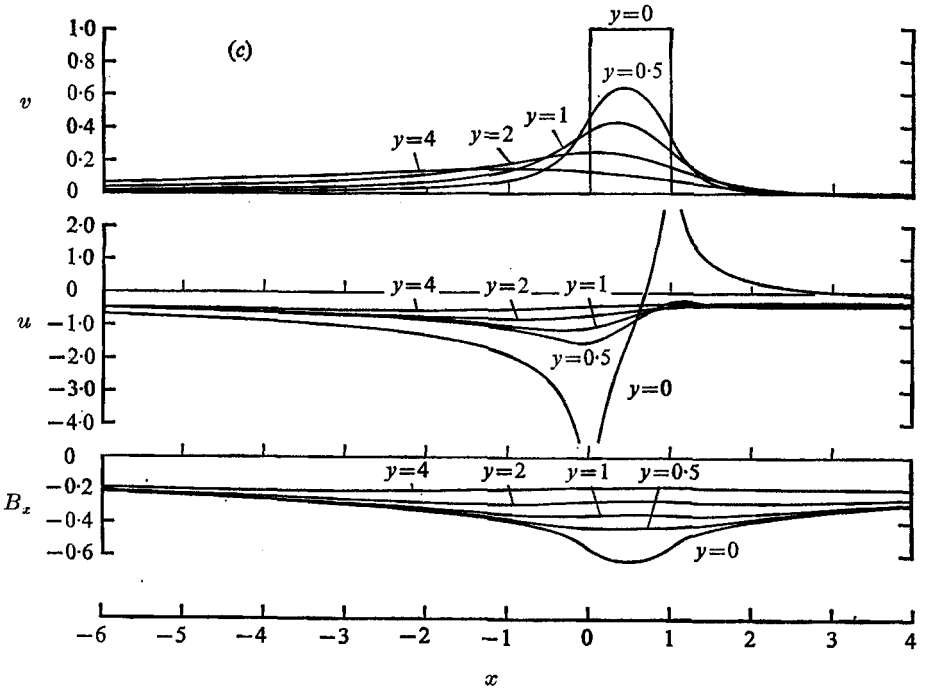

FIGURE 1. Distributions of v, u and B_x for insulator and $N = 1$. (*a*) $M^2 = 2$, $A^2 = 0{\cdot}5$. (*b*) $M^2 = 4$, $A^2 = 1{\cdot}5$. (*c*) $M^2 = A^2 = 0{\cdot}6$.

Two cases are distinguished according as the wedge consists of an insulator or perfect conductor. Three typical flows are considered:

$$(a)\ M^2 = 2, \quad A^2 = 0{\cdot}5;$$

$$(b)\ M^2 = 4, \quad A^2 = 1{\cdot}5;$$

$$(c)\ M^2 = 0{\cdot}6, \quad A^2 = 0{\cdot}6.$$

Flow (*a*) is hyperbolic in type at the limit $R_m \to 0$ and elliptic at the limit $R_m \to \infty$. Flow (*c*), conversely, is elliptic in type in the limit $R_m \to 0$ and hyperbolic in the limit $R_m \to \infty$. Flow (*b*) is of hyperbolic type in both limits, but the characteristics are in different directions. The values of the interaction parameter N are taken as 1 and 10 for the insulator and as 1 for the perfect conductor. The results are shown as distributions of v, u and B_x along several streamlines for the above three flows in figures 1 ($N = 1$, insulator), 2 ($N = 10$, insulator) and 3 ($N = 1$, perfect conductor).

The calculation is based on the approximate evaluation of the Fourier integrals by dividing them into trapezoidal strips. However, if the integrand behaves like $\xi^{-1}\sin(a\xi)$ or $\xi^{-1}\sin(a\xi)\sin(b\xi)$ for large values of ξ, the calculation is performed for the integrand minus its asymptotic function and then the function $\frac{1}{2}\pi\,\mathrm{sgn}(a)$ or $\frac{1}{2}\ln|(a+b)/(a-b)|$ is added to its result. Further, if the integrand has a singularity such as $\xi^{-\frac{1}{2}}$ at $\xi = 0$, the analytically evaluated value from the expansion about $\xi = 0$ is used for the first interval. The intervals are of the equal

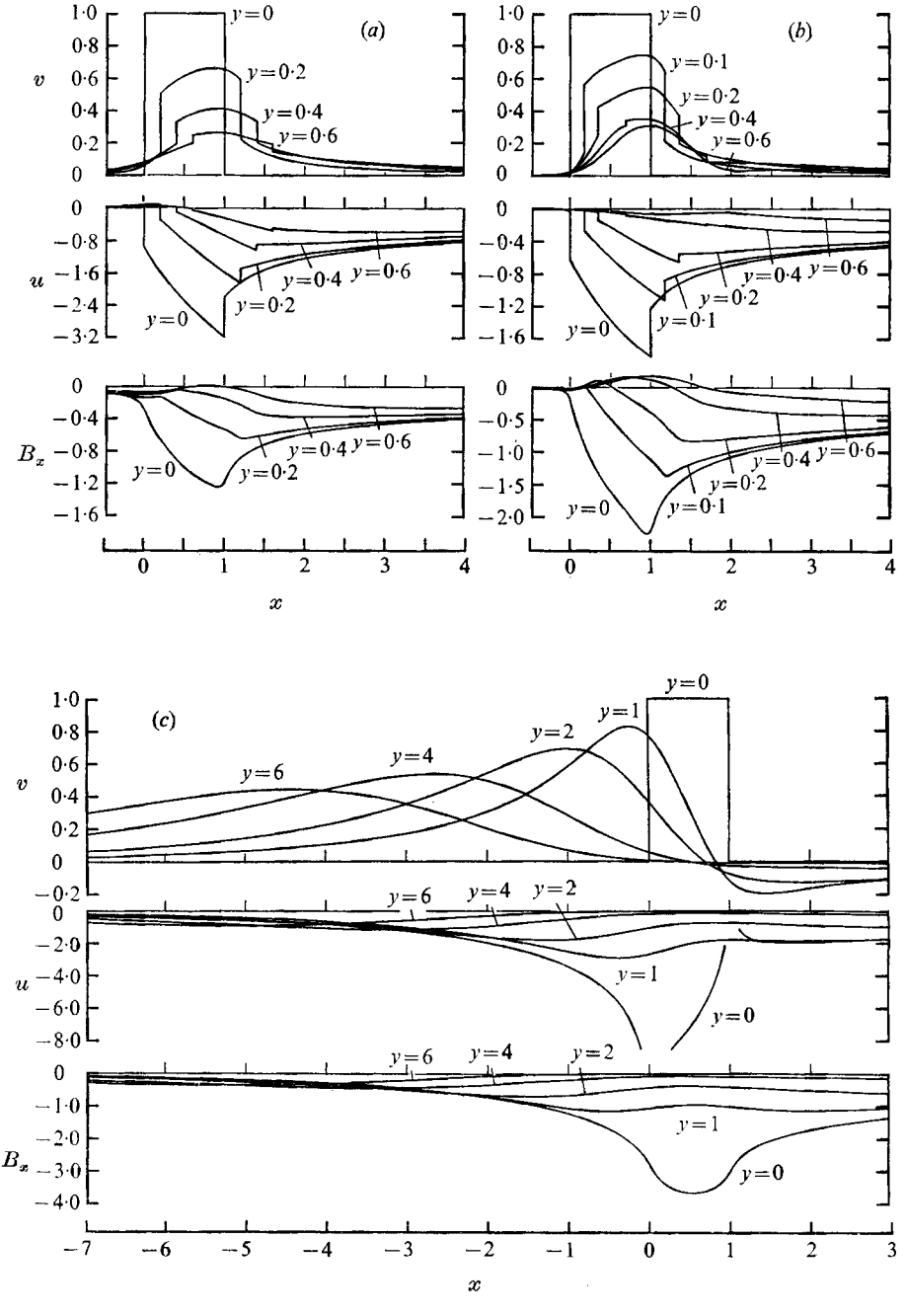

FIGURE 2. Distributions of v, u and B_x for insulator and $N = 10$. (*a*) $M^2 = 2$, $A^2 = 0{\cdot}5$. (*b*) $M^2 = 4$, $A^2 = 1{\cdot}5$. (*c*) $M^2 = A^2 = 0{\cdot}6$.

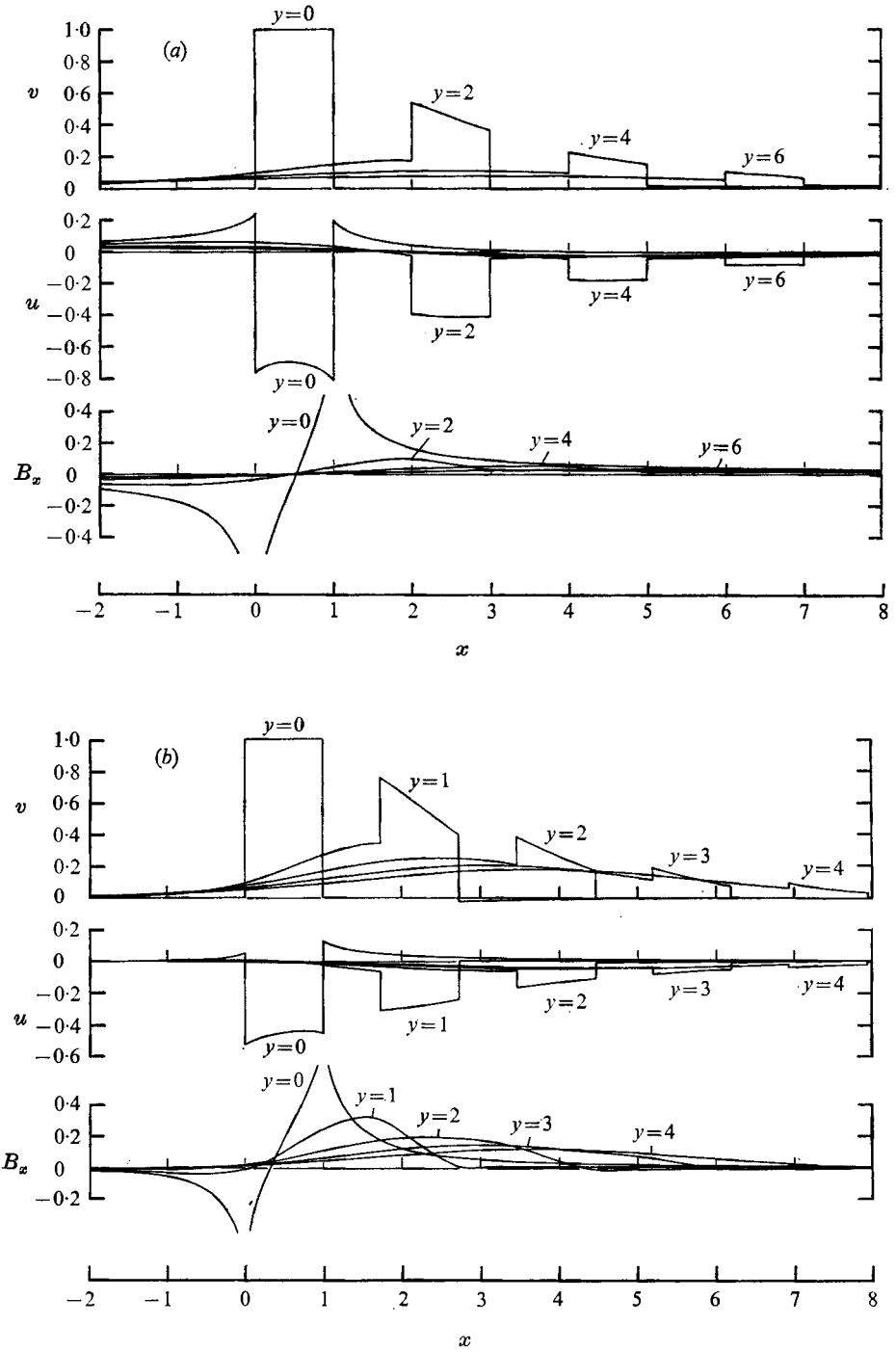

FIGURES 3 (*a*, *b*). For legend see next page.

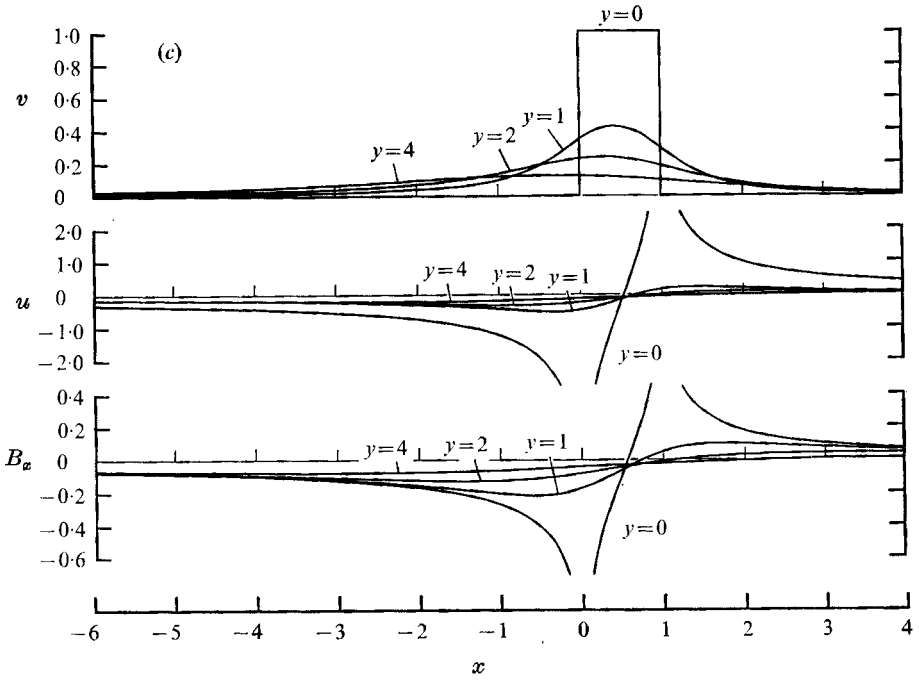

FIGURE 3. Distributions of v, u and B_x for perfect conductor and $N = 1$. (*a*) $M^2 = 2$, $A^2 = 0{\cdot}5$. (*b*) $M^2 = 4$, $A^2 = 1{\cdot}5$. (*c*) $M^2 = A^2 = 0{\cdot}6$.

length 0·01, and contributions are taken into account from $\xi = 0$ to 10 if the integrand includes an effectively operating exponential term, and from $\xi = 0$ to 30 or 80 for the other cases.

First we consider the results of the insulator. In flows (*a*) and (*b*), we can find the gasdynamic shock waves starting from the nose. They have the same velocity jump as in the pure gasdynamic case at the nose, but they decay with a distance from the nose and the flow behind them is no longer uniform owing to the Lorentz force. In fact, by expanding the integrand in (20) for large ξ and taking into account only the contribution from the most dominant term, we can deduce that such a decay of the shock strength is proportional to $\exp(-\frac{1}{2}m^{\frac{1}{2}}Ny)$ (Morioka 1967). A similar discussion is possible for the expansion wave starting from the shoulder. In flow (*c*), on the other hand, the perturbation velocity u on the surface shows a logarithmic singularity at the nose and shoulder, as in the subsonic flow in ordinary gasdynamics. Thus, the flow field near the wedge retains the gasdynamical features, but they disappear with distance and there remains the flow with magnetohydrodynamic properties. Comparing the results for $N = 1$ and 10, we can find how such a transition is improved by increasing N. In flows (*b*) and (*c*), we may notice the growth of a magnetohydrodynamic shock layer downstream or upstream.

The perturbation density has the same distribution profile as the perturbation velocity u from (5). The distribution profiles of the magnetic field evidently have no discontinuity in any of the flows, but there are remarkable differences between

those in supersonic and subsonic flows. The abrupt change of the profiles near the surface, evident in the figures for $N = 10$, suggests the growth of a magnetohydrodynamic boundary layer, which will significantly influence the outer flow as discussed in the previous section. However, further discussions for larger N are impossible within the present linearized theory.

For the ideal case of a perfect conductor, the magnetic field cannot penetrate into the obstacle and runs along the surface. Thus, the distribution profile of the magnetic field is different from that in the insulator. In particular, the profile on the surface has cusps at the nose and shoulder. Their values are finite but somewhat large. Thus the flow also may be different from that in the insulator, owing to the interaction with such a magnetic field. In fact, we can find a conspicuous leak ahead of the shock wave in the supersonic flow. From the asymptotic expansion of (20) for large ξ or the series approximation of (1)–(4) for small N, we can show that such a leak is of $O(N)$ for the perfect conductor, and $O(N^2)$ for the insulator. Nevertheless, the gasdynamic features such as shock jump or logarithmic singularity at the nose and shoulder are still retained. They disappear at large distances from the obstacle and a flow with magnetohydrodynamic features such as a diffused shock layer appears.

Finally, we may notice that, from the above figures, the upstream shock wave will be produced more strongly by the insulator wedge, and the downstream shock wave by the perfect conductor.

REFERENCES

ERDÉLYI, A. 1956 *Asymptotic Expansions*. Dover.
IMAI, I. 1960 *Rev. Mod. Phys.* **32**, 992.
MCCUNE, J. E. & RESLER, E. L. 1960 *Aerospace Sci.* **27**, 493.
MORIOKA, S. 1967 *J. Phys. Soc. Japan*, **22**, 1471.
RESLER, E. L. & MCCUNE, J. E. 1960 *Rev. Mod. Phys.* **32**, 848.
SAKURAI, T. 1960 *J. Phys. Soc. Japan*, **15**, 326.
SEARS, E. R. & RESLER, E. L. 1959 *J. Fluid Mech.* **5**, 257.
TAMADA, K. 1962 *Phys. Fluids*, **8**, 871.